

KINEMATIC CONTROL OF A NONHOLONOMIC WHEELED MOBILE MANIPULATOR – A DIFFERENTIAL FLATNESS APPROACH

Chin Pei Tang, Patrick T. Miller, Venkat N. Krovi
Department of Mechanical & Aerospace Engineering
University at Buffalo
318 Jarvis Hall
Buffalo NY 14260
chintang,pmiller4,vkrovi@buffalo.edu

Ji-Chul Ryu, Sunil K. Agrawal
Department of Mechanical Engineering
University of Delaware
126 Spencer Lab
Newark DE 19716
jcryu,agrawal@udel.edu

ABSTRACT

This paper presents an integrated motion planning and control framework for a nonholonomic wheeled mobile manipulator (WMM) system taking advantage of the (differential) flatness property. We first develop the kinematic model of the system and analyze its flatness properties. Subsequently, a statically feedback linearizable system description is developed by appropriately choosing the flat outputs. Motion-planning can now be achieved by polynomial curve fitting to satisfying the terminal conditions in the flat output space while control design reduces to a pole-placement problem for a linear system. A case study of point-to-point motion is considered to study the effectiveness of pose stabilization in the WMM. The simulation and experimental results highlight the ease-of-implementation of proposed method for online real-time integrated motion-planning/control within a hardware-in-the-loop (HIL) electro-mechanical testing.

NOMENCLATURE

WMR Wheeled Mobile Robot
WMM Wheeled Mobile Manipulator
 (x, y) Cartesian coordinates of the center of the wheel axle of the WMR
 φ Orientation of the WMR with respect to the global frame
 θ_1, θ_2 Relative angles to describe the configuration of the two-link manipulator
 θ_r, θ_l Angular positions of the right and left wheel, respectively
 v, ω Forward and angular velocity inputs to WMR

u_1, u_2 Velocity inputs to first and second joints of the manipulator, respectively
 η Acceleration of the WMR, $\eta = \dot{v}$
 q Vector of generalized coordinates of the system.
 F Flat outputs
 $F(t)$ Actual trajectories in the flat output space
 $F^d(t)$ Desired trajectories in the flat output space
 ξ Change of inputs for feedback linearization
 e Error between the desired and the actual trajectories in the flat output space
 T Final time

1. INTRODUCTION

Partially or fully-autonomous robotic systems have proven very useful in extending the reach and capabilities of humans in numerous manipulation and environment-interaction tasks. The archetypical robotic system with a fixed-base manipulator possesses considerable manipulation capabilities but a bounded (and thereby) limited workspace. However, mounting such a manipulator on a mobile base creates the so-called mobile manipulator configuration with novel capabilities endowed by the merger of mobility with manipulation. Numerous applications, ranging from gantry-mounted manipulators on the shop floor to highway maintenance robots to robotic earth-moving excavators to free-flying satellite-repair robots, have capitalized on this merger. The benefits included expanded workspace (both conventional and dexterous), reconfigurability, improved disturbance-rejection capabilities and robustness to failure [1-6].

Many variants are possible based on the nature of the mobile base (gantry system, another manipulator or some wheeled or tracked platform) and the nature of the mounted manipulator (number and actuation of the articulations). In this paper, we focus on the subclass of wheeled mobile manipulator (WMM) consisting of a wheeled mobile robot (WMR) with mounted multi-degree-of-freedom (DOF) manipulator. While robust physical construction, ease of addition to platforms and ease of operation make disk wheels popular, the kinematics of rolling contact creates nonholonomic constraints and the resulting class of nonholonomic WMMs requires special treatment. Motion planning and control of a nonholonomic system is generally more difficult due to the existence of nonintegrable rate constraints in the configuration space – see [7, 8] for review.

Numerous studies have found on motion planning and control of nonholonomic WMMs. Yamamoto and Yun [6] showed that a WMM system is not input-state linearizable by static state feedback, but is input-output linearizable by appropriate selection of output coordinates. Seraji [3] presents a unified kinematic redundancy resolution framework within explicit distinction of WMR and manipulator subsystems. Bayle et. al. [9] extended such redundancy resolution framework by incorporating the idea of “preferred configuration” approach using manipulability similarly in [6]. Fruchard et al. [10] presents a general kinematic control framework of WMM based on the transverse function approach such that it is independent of the mobile base configuration. However, no prior work has considered the exploitation of differential flatness, with its many merits, in the context of WMMs. The problem can be considerably simplified if the system exhibits differential flatness characteristics, which was first investigated by Fliess *et al.* [11]. Murray *et al.* [12] provided an alternative characterization to such flatness properties for Lagrangian mechanical system in a differential geometric framework and created an initial catalog of existing differentially flat systems. The book by Sira-Ramirez and Agrawal [13] summarizes the diversity and greater number of engineering applications that could be analyzed using the differential flatness characteristics.

To succinctly summarize: by virtue of the flatness approach, the states and inputs can be parameterized by a finite set of independent variables, called the flat outputs, and their (time) derivatives. Moreover, the number of flat outputs is equal to the number of control inputs. This enables the transformation of nonlinear differential equations into a system of algebraic equations which are, in general, simpler to solve. Hence, differential flatness is useful for trajectory planning problem since the desired trajectory can be planned in flat output space algebraically, using a variety of interpolating functions (including polynomials of appropriate order, as we do in this paper) to match terminal conditions. In addition, exponential stabilizing controllers can be

developed since in the flat output space, the system has the representation of a chain of integrators. There have been a few recent studies on mobile robotics using such methods, including [14-16]. However, in this paper, we explore the use of such method to the case of a full WMM. Further, except [6], not much experimental evaluation have been performed. Based on our experience [17], although many different high-level unified control laws exist, they are still considerably sensitive when evaluated on experimental hardware.

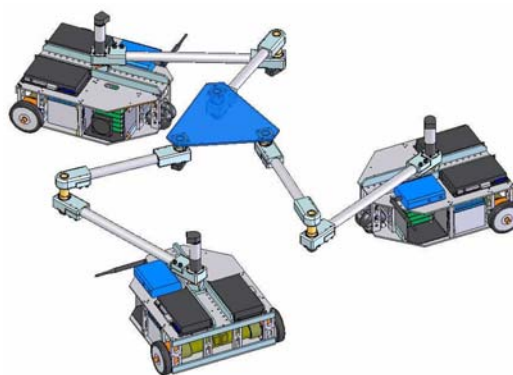


FIGURE 1. A COLLECTIVE OF WHEELED MOBILE MANIPULATORS COOPERATIVELY TRANSPORT A COMMON PAYLOAD

Our ultimate overall goal is to develop a framework to achieve cooperative payload transport using multiple WMM (as shown in Figure 1). Consider the following illustrative scenario wherein multiple WMMs attach themselves to a payload at a predetermined configuration (to achieve highest cooperative level manipulability [18]). The WMMs may be initially parked statically in the warehouse and given the initial and final configuration, the goal is to develop an integrated motion planning/control strategy to achieve such a point-to-point motion. Hence, *the contribution of the paper is to present a simple solution to achieve the initial point-to-point motion by utilizing the differential flatness approach to realize the subsequent cooperative payload transport operation and validate the applicability of the framework using a hardware-in-the-loop experimentation.*

The rest of the paper is organized as follows: Section 2 develops the notation and the kinematic model for the WMM under consideration. Section 3 focuses on creation of a kinematic control law based on the differential flatness property of the system. Section 4 develops the simple point-to-point polynomial-based motion planner. Section 5 describes the electromechanical hardware and the overall framework used to develop and evaluate the controller. Section 6 presents both simulation and experimental results to show the effectiveness of the motion planning/control scheme. Section 7 concludes the paper with a brief discussion and summarizes the avenues for future work.

2. KINEMATIC MODEL

In this section, we present the notation and the kinematic model of the system under consideration. Referring to Figure 2, the WMM under consideration consists of a differentially driven WMR base with a mounted planar two-link RR manipulator. The wheels are located at a distance of b from the center of the wheel axle. The wheel has a radius of r . The base of the manipulator is located at a distance of L_a from the center of the wheel axle. The length of the first and second links are L_1 and L_2 respectively.

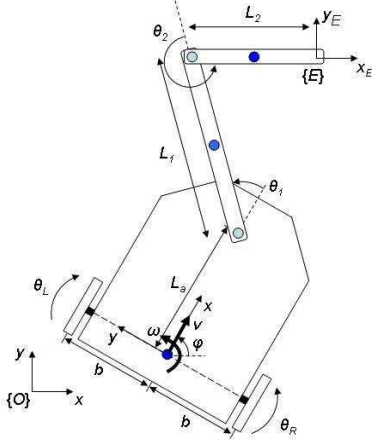


FIGURE 2. SCHEMATIC OF THE WHEELED MOBILE MANIPULATOR UNDER CONSIDERATION

The configuration of a WMM can be completely described by the following generalized coordinates:

$$q^T = [q_B^T \ q_M^T] = [x \ y \ \varphi \ \theta_1 \ \theta_2] \quad (1)$$

where $q_B^T = [x \ y \ \varphi]$ describes the configuration of the WMR and $q_M^T = [\theta_1 \ \theta_2]$ describes the configuration of the planar manipulator. (x, y) is the Cartesian position of the center of the axle of the WMR, φ is the orientation of the WMR, and θ_1, θ_2 are the relative angles that parameterize the first and second link of the mounted manipulator. The kinematics of the differentially-driven WMR can be represented by its equivalent unicycle model, and described as:

$$\begin{bmatrix} \dot{x} \\ \dot{y} \\ \dot{\varphi} \end{bmatrix} = \begin{bmatrix} \cos \varphi & 0 \\ \sin \varphi & 0 \\ 0 & 1 \end{bmatrix} \begin{bmatrix} v \\ \omega \end{bmatrix} \quad \text{or} \quad \dot{q}_B = J_B u_B \quad (2)$$

where v and ω are the forward and angular velocities inputs. To extend to the mobile manipulator case, we simply extend the kinematics of the entire system to:

$$\begin{bmatrix} \dot{q}_B \\ \dot{q}_M \end{bmatrix} = \begin{bmatrix} J_B & 0 \\ 0 & I \end{bmatrix} \begin{bmatrix} u_B \\ u_M \end{bmatrix} \quad (3)$$

where $u_M^T = [u_1 \ u_2]$ are the joint velocity input to the individual manipulator joints.

3. DIFFERENTIAL FLATNESS BASED CONTROLLER

Considering only the WMR model in (2), it can be shown that the system cannot be (exactly) statically feedback linearized. Specifically, if we define the flat outputs to be:

$$F_B^T = [F_1 \ F_2] = [x \ y] \quad (4)$$

and differentiate with respect to time:

$$\dot{F}_B = \begin{bmatrix} \dot{F}_1 \\ \dot{F}_2 \end{bmatrix} = \begin{bmatrix} \dot{x} \\ \dot{y} \end{bmatrix} = \begin{bmatrix} \cos \varphi & 0 \\ \sin \varphi & 0 \end{bmatrix} \begin{bmatrix} v \\ \omega \end{bmatrix} \quad (5)$$

The mapping between the input to the flat outputs turns out to be singular, i.e. the information of ω cannot be recovered from the relationship. The method to address this problem is to introduce the input prolongation of v (extending v as a state), and the extended system can be described as:

$$\dot{x} = v \cos \varphi, \dot{y} = v \sin \varphi, \dot{v} = \eta, \dot{\varphi} = \omega \quad (6)$$

where η is the new (forward acceleration) input to the system and the accelerations of the flat output are:

$$\ddot{F}_B = \begin{bmatrix} \ddot{F}_1 \\ \ddot{F}_2 \end{bmatrix} = \begin{bmatrix} \ddot{x} \\ \ddot{y} \end{bmatrix} = \begin{bmatrix} \cos \varphi & -v \sin \varphi \\ \sin \varphi & v \cos \varphi \end{bmatrix} \begin{bmatrix} \eta \\ \omega \end{bmatrix} \quad (7)$$

In this case, the mapping is singular if $v=0$, and we avoid this situation in our case. Hence, effectively, the modified output of the system is the forward acceleration η and the angular velocity ω of the robot. For the manipulator, we can choose the flat outputs to be:

$$F_M^T = [F_3 \ F_4] = q_M^T = [\theta_1 \ \theta_2] \quad (8)$$

Hence, the complete set of flat outputs $F^T = [F_B^T \ F_M^T]$ can now be completely expressed by the system states, the inputs and the time derivatives as:

$$\begin{aligned} F_1 &= x, F_2 = y, F_3 = \theta_1, F_4 = \theta_2, \\ \dot{F}_1 &= \dot{x} = v \cos \varphi, \dot{F}_2 = \dot{y} = v \sin \varphi, \\ \dot{F}_3 &= u_1, \dot{F}_4 = u_2, \\ \ddot{F}_1 &= \dot{v} \cos \varphi - v \omega \sin \varphi, \\ \ddot{F}_2 &= \dot{v} \sin \varphi + v \omega \cos \varphi \end{aligned} \quad (9)$$

Conversely, the states and the inputs can also be expressed completely by the flat outputs (and their time derivatives) as:

$$\begin{aligned}
x &= F_1, y = F_2, \varphi = \text{atan}(\dot{F}_2, \dot{F}_1), \\
v &= \sqrt{\dot{F}_1^2 + \dot{F}_2^2}, \omega = \frac{\dot{F}_1 \ddot{F}_2 - \dot{F}_2 \ddot{F}_1}{\dot{F}_1^2 + \dot{F}_2^2}, \\
\eta &= \frac{\dot{F}_1 \ddot{F}_1 + \dot{F}_2 \ddot{F}_2}{\sqrt{\dot{F}_1^2 + \dot{F}_2^2}}, \\
\theta_1 &= F_3, \theta_2 = F_4, \\
\dot{\theta}_1 &= u_1 = \dot{F}_3, \dot{\theta}_2 = u_2 = \dot{F}_4
\end{aligned} \tag{10}$$

The system (9) can be linearized using the following change of inputs:

$$\ddot{F}_1 = \xi_1, \ddot{F}_2 = \xi_2, \dot{F}_3 = \xi_3, \dot{F}_4 = \xi_4 \tag{11}$$

Given desired trajectories of the flat outputs $F_1^d(t)$, $F_2^d(t)$, $F_3^d(t)$, $F_4^d(t)$, the control laws to the new inputs can then be defined as:

$$\begin{aligned}
\xi_1 &= \ddot{F}_1^d + p_1(\dot{F}_1^d - \dot{F}_1) + p_2(F_1^d - F_1) \\
\xi_2 &= \ddot{F}_2^d + q_1(\dot{F}_2^d - \dot{F}_2) + q_2(F_2^d - F_2) \\
\xi_3 &= \dot{F}_3^d + r_1(F_3^d - F_3) \\
\xi_4 &= \dot{F}_4^d + s_1(F_4^d - F_4)
\end{aligned} \tag{12}$$

The corresponding linearized (error) dynamics can then be written as:

$$\begin{aligned}
\ddot{e}_1 + p_1 \dot{e}_1 + p_2 e_1 &= 0, \dot{e}_3 + r_1 e_3 = 0 \\
\ddot{e}_2 + q_1 \dot{e}_2 + q_2 e_2 &= 0, \dot{e}_4 + s_1 e_4 = 0
\end{aligned} \tag{13}$$

where $e_i = F_i^d - F_i$, $i = 1, 2, 3, 4$. By suitably selected gains, the linear error dynamic in (13) can be exponentially driven to zero. Substituting (12) into (11), the original required inputs ω, u_1, u_2 to the system can then be determined using (10). However, the input $\eta = \dot{v}$ has to be integrated with respect to time to obtain v . The corresponding right and left wheel angular velocities ($\dot{\theta}_r$ and $\dot{\theta}_l$ respectively) can be obtained from v and ω as:

$$\begin{bmatrix} \dot{\theta}_r \\ \dot{\theta}_l \end{bmatrix} = \frac{1}{r} \begin{bmatrix} 1 & b \\ 1 & -b \end{bmatrix} \begin{bmatrix} v \\ \omega \end{bmatrix} \tag{14}$$

Note also that the inverse of this mapping can be used to transform the wheel velocity readings back to the corresponding v and ω as:

$$\begin{bmatrix} v \\ \omega \end{bmatrix} = \frac{r}{2} \begin{bmatrix} 1 & 1 \\ \frac{1}{b} & -\frac{1}{b} \end{bmatrix} \begin{bmatrix} \dot{\theta}_r \\ \dot{\theta}_l \end{bmatrix} \tag{15}$$

4. POINT-TO-POINT MOTION PLANNING

For illustration purposes, we present a simple polynomial-based trajectory planning for a set of given terminal conditions. Since the extended state space and the flat output space have one-to-one mapping from (9) and (10), the trajectory can be planned algebraically in the flat output space. For the time interval $t \in [0, T]$, given the terminal conditions:

$$\begin{aligned}
&x(0), y(0), \varphi(0), v(0), \eta(0), \omega(0), \theta_1(0), \theta_2(0), \dot{\theta}_1(0), \dot{\theta}_2(0) \\
&x(T), y(T), \varphi(T), v(T), \eta(T), \omega(T), \theta_1(T), \theta_2(T), \dot{\theta}_1(T), \dot{\theta}_2(T)
\end{aligned}$$

They can be transformed to the corresponding terminal conditions in the flat outputs of:

$$\begin{aligned}
&F_1(0), \dot{F}_1(0), \ddot{F}_1(0), F_2(0), \dot{F}_2(0), \ddot{F}_2(0), F_3(0), \dot{F}_3(0), F_4(0), \dot{F}_4(0) \\
&F_1(T), \dot{F}_1(T), \ddot{F}_1(T), F_2(T), \dot{F}_2(T), \ddot{F}_2(T), F_3(T), \dot{F}_3(T), F_4(T), \dot{F}_4(T)
\end{aligned}$$

Taking the trajectories in the form of:

$$\begin{aligned}
F_1^d(t) &= a_1 t^3 + a_2 t^2 + a_3 t + a_4, F_3^d(t) = c_1 t + c_2 \\
F_2^d(t) &= b_1 t^3 + b_2 t^2 + b_3 t + b_4, F_4^d(t) = d_1 t + d_2
\end{aligned} \tag{16}$$

The coefficients of the polynomials can be determined uniquely using the terminal conditions. Hence, any arbitrary trajectories of $F_1(t)$, $F_2(t)$, $F_3(t)$, $F_4(t)$ can be constructed in the flat output space, provided that each of the trajectory satisfies the terminal conditions.

5. EXPERIMENTAL HARDWARE DESCRIPTION

We employ a *hardware-in-the-loop* (HIL) methodology for rapid experimental verification of the real-time controllers on the electromechanical mobile manipulators prototypes. We opted to create a physical WMM system from scratch due to the flexibility it offered over retrofitting an off-the-shelf WMR base with an off-the-shelf manipulator arm – see Figure 3(A). The physical dimensions of the system are tabulated in Table 1. The WMM is constructed using two powered wheels and one passive MECANUM-type casters. Conventional disc-type rear wheels, powered by two Pitman gear-motors, are chosen because of robust physical construction and ease of operation in the presence of terrain irregularities. Optical encoders at the motors provide the encoder feedback and odometer for the base platform. A passive MECANUM-type front caster was preferred (over a conventional wheel casters) to eliminate any constraints on the maneuverability. The mounted manipulator arm has two active revolute joints with axes of rotation parallel to each other and perpendicular to the mobile platform (and the ground). The first joint can be placed anywhere along the mid-line on top frame of the platform at the distance of L_a from the mid-point of the wheel axle – see Figure 2. The lengths of the first and second links can be freely adjusted by changing the length of the connecting rod. The two joints are

also instrumented with optical encoders that can measure the joint rotations and have Maxon DC motors attached. Independent lead-acid batteries provide power supplies for the actuator systems and the electronic-controllers.

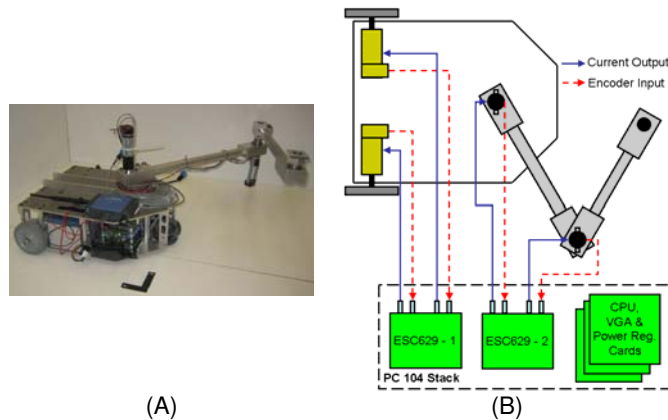


FIGURE 3. (A) EXPERIMENTAL ELECTRO-MECHANICAL PROTOTYPE, AND (B) LAYOUT OF THE ELECTRONICS INVOLVED IN THE PC/104 SYSTEM OF THE WMM UNDER CONSIDERATION

TABLE 1. PHYSICAL DIMENSIONS OF THE WMM

Parameters	Variables	Values	Units
Half distance between the two wheels	b	0.182	m
Radii of the wheels	r	0.0508	m
Distance from CM of the mobile base to the base of the manipulator	L_a	0.216	m
Length of Link 1	L_1	0.508	m
Length of Link 2	L_2	0.362	m

A PC/104 system, equipped with an xPC Target Real-Time Operating System (RTOS) serves as the embedded controller. A PC104+ embedded computer (VersaLogic EPM-CPU-3 133MHz 32-bit processor with standard PC I/O and 10/100 Ethernet) is used to do all high-level processing, control, and communication onboard the robot. Wireless communication is accomplished with a standard Linksys wireless Ethernet bridge. The host computer is running MATLAB/Simulink/Real Time Workshop, a convenient graphical interface supporting block based control design, code compilation and host/target communication. Compiled C code as well as real-time data can be transferred back and forth between the host and target computer using the TCP/IP connection. Code downloaded to the embedded controller can directly access the local hardware. This provides the ability to test the individual hardware components of the system (i.e. individual motors and encoders) or the entire unit at once. The individual motors are controlled using ESC629, a 2-channel DC servo motor interface board with an on-board incremental encoder input and PID gain tunings. The electronics layout is depicted in Figure 3(B).

6. SIMULATION AND EXPERIMENTAL RESULTS

We show 3 case studies to demonstrate the effectiveness of the proposed framework, both in terms of preliminary simulations (in MATLAB/Simulink), and the direct conversion to the HIL testing for the hardware prototype, as described in the previous section.

6.1. Case I: Simulation Results of Initial Error Compensation for Single WMM

In the first case, we plan the desired trajectories for $T = 30s$. To achieve point-to-point motion, we required all the terminal velocity conditions to be zero, except the quantity v , which we kept to be a small number to avoid singularity. For the position variables, we plan the trajectories according to the following desired conditions¹:

$$\begin{aligned} x^d(0) &= 0.0m, y^d(0) = 0.0m, \varphi^d(0) = 0^\circ, \theta_1^d(0) = 60^\circ, \theta_2^d(0) = 60^\circ \\ x^d(T) &= 1.5m, y^d(T) = 1.0m, \varphi^d(T) = 0^\circ, \theta_1^d(T) = 45^\circ, \theta_2^d(T) = 90^\circ \end{aligned}$$

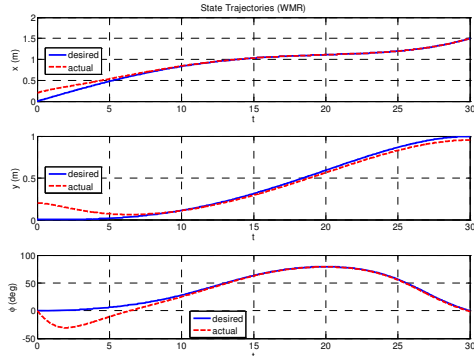
It is worth noting that the desired final configuration of the WMM is such that at the highest manipulability at the end-effector (using the results from [6]) when reaching the final condition. In order to evaluate the effectiveness of the control, we impose an initial configuration error for the WMM, where the actual initial conditions are²:

$$x^a(0) = 0.2m, y^a(0) = 0.2m, \varphi^a(0) = 0^\circ, \theta_1^a(0) = 70^\circ, \theta_2^a(0) = 65^\circ$$

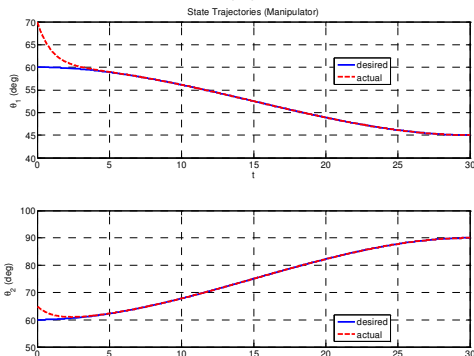
Figure 4(A) and (B) depict the desired and the actual state trajectories of the motion of the WMM. Figure 4(C) shows the screenshots of the WMM moving from left to right, and plotting at the frame rate of 1 frame per 5 seconds. The desired and the actual trajectories of the WMR are also superimposed in the graph. It is observed that despite the initial error, the WMM is able to (exponentially) converge to the desired trajectory after the initial transient. The transient is depending on the selection of gains for the error dynamics in (13). In our case, we selected the gains such that the error transients are overdamped. However, the selection of the gains cannot be arbitrary, a fact that is often ignored by many analyses in the literature. Due to the existence of velocity saturation of each actuator, we plot the angular velocity inputs of each actuator. By carefully selecting the gains, we are able to make sure the required velocity input stay within the limit of the motors – see Figure 4(D). Another important factor that would affect the resulting required velocity input is the time taken T to achieve the required desired final configuration. If T is chosen to be small (fast stabilization), the required input would be much demanding. Hence, the control designer should also be careful in deciding the time required to achieve the final configuration such that the required input profile stays within the hardware limit.

¹ Superscript d indicates the “desired” planned trajectory.

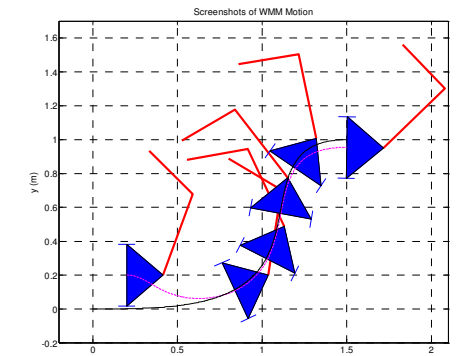
² Superscript a indicates the “actual” motion of the trajectory.



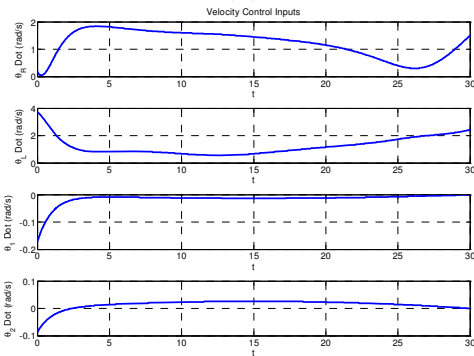
(A)



(B)

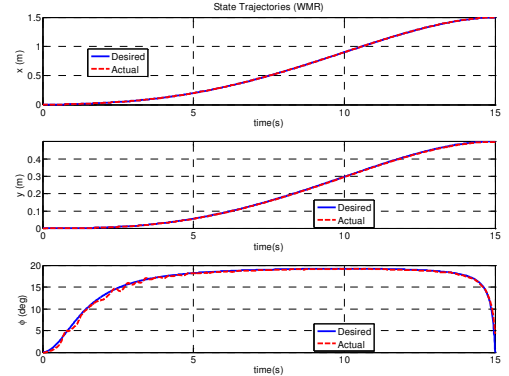


(C)

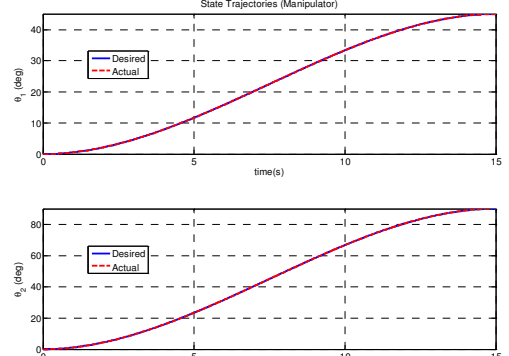


(D)

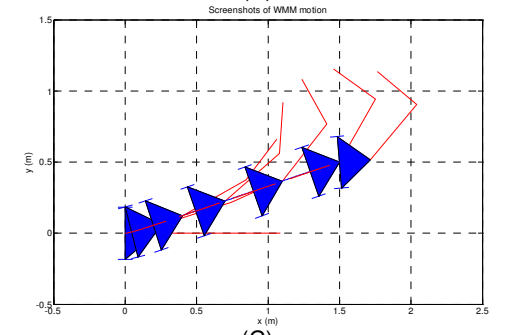
FIGURE 4. CASE I – SIMULATION RESULTS: (A) THE STATE TRAJECTORIES OF THE WMR, (B) THE STATE TRAJECTORIES OF THE MANIPULATOR, (C) THE SCREENSHOTS OF THE WMM MOTION, AND (D) THE ANGULAR VELOCITY INPUT TO EACH ACTUATOR



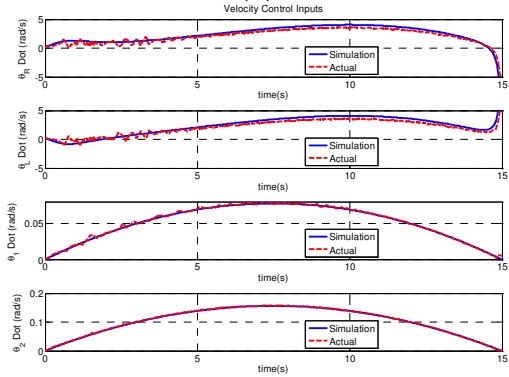
(A)



(B)



(C)



(D)

FIGURE 5. CASE II – EXPERIMENTAL RESULTS: (A) THE STATE TRAJECTORIES OF THE WMR, (B) THE STATE TRAJECTORIES OF THE MANIPULATOR, (C) THE SCREENSHOTS OF THE WMM MOTION, AND (D) THE ANGULAR VELOCITY INPUT TO EACH ACTUATOR

6.2. Case II: Experimental Results of Tracking of Single WMM

We then evaluate the controller using the experimental framework described in the previous section. Due to the workspace limitation in the lab, we run the experiments under the following conditions with $T = 15s$:

$$\begin{aligned} x^d(0) &= 0.0m, y^d(0) = 0.0m, \varphi^d(0) = 0^\circ, \theta_1^d(0) = 0^\circ, \theta_2^d(0) = 0^\circ \\ x^d(T) &= 1.5m, y^d(T) = 0.5m, \varphi^d(T) = 0^\circ, \theta_1^d(T) = 45^\circ, \theta_2^d(T) = 90^\circ \end{aligned}$$

We then compare the experimental results with the simulated results. Figure 5(A) and (B) shows the state trajectories of the motion of the WMM computed from the encoder readings, and compared with the desired/simulated results. Figure 5(C) shows the screenshots of the corresponding motion. Since the quantity φ is not directly a measured quantity (not a flat output), it is very sensitive to the odometry (velocity) data from the wheels. From the third subplot of Figure 5(A) (and also the final configuration shown in Figure 5(C)), the final angular quantity has a small error. Furthermore, the selection of the gain for the second flat output, namely $F_2 = y$ is also sensitive due to the existence of the nonholonomic constraints in the y - direction. While the final configuration is achieved closely, the resulting hardware is reasonably sensitive to the selection of control gains especially for the base. If the gains are selected to be too high, it requires very high v and ω inputs (and the corresponding input wheel velocities $\dot{\theta}_r$ and $\dot{\theta}_l$) which destabilizes the hardware. If the gains are selected to be too low, the desired y might not achieve accurately. Figure 5(D) shows the input velocities to the system. It can also be seen that the required actual inputs profiles follow closely to the simulated input profiles, which verified the applicability of such approach.

6.3. Case III: Simulation Results of Multiple WMMs Moving Towards a Common Payload

Our major goal is to have multiple WMMs carry a payload (like an “army of ants” come together to carry a large food morsel). In this case study, we require the WMM modules to start from an initial rest configuration (say parked in the warehouse), and come together to the final configuration to attach at the payload. Figure 6 shows screenshots of such an operation. In this case, the 3 WMMs (labeled WMM A, WMM B and WMM C) are aligned at the left corner (in the warehouse). The WMMs are required to achieve the final configurations to attach at the payload in $T = 30s$. Each robot trajectory is designed using the differential flatness framework described before. We also assumed that the robots are homogeneous (the robots have the same geometry and hardware capability). They used the exact same planning/control algorithms – hence the method can potentially be “parallelized” in terms of computation

once the final configuration is known and broadcasted. The figure shows one intermediate screenshot (at $t = 15s$) while each of the robot tracking their individual required trajectory (x, y coordinates of the wheel center is superimposed in the graph), and the final configuration attaching the payload.

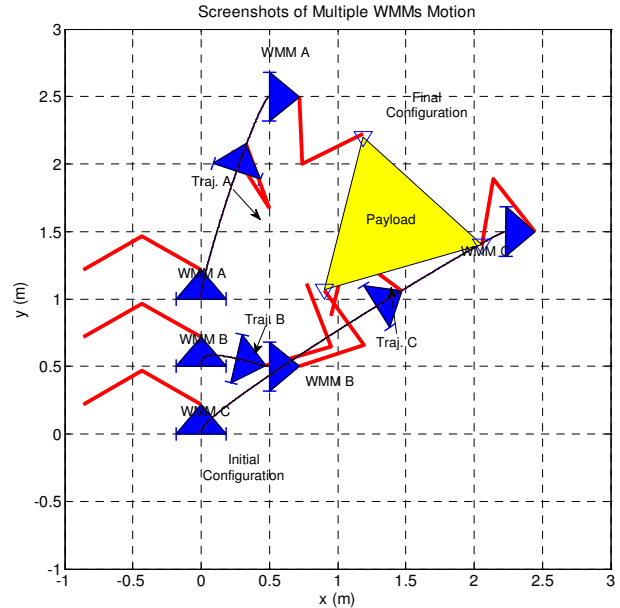


FIGURE 6. CASE III - MULTIPLE WMMs STARTED FROM PARKED POSITION, MOVING TOWARDS AND ATTACHING THE PAYLOAD USING THE DIFFERENTIAL FLATNESS METHOD

The case study in this case is preliminary, and we use this case to highlight some of the potential open problems that can be pursued in the future. As noticed in the figure, WMM C is colliding with the payload during the tracking. Such situation can be avoided by using a higher order polynomial trajectory (or Bezier curve). Furthermore, during the maneuver, WMM B can potentially collide with WMM C. One resolution method may be to assign priorities to the robots – WMM C should go first before WMM B – but such a discussion is beyond the scope of this paper.

7. CONCLUSION

In this paper, we showed that the WMM system is differentially flat in the kinematic model if the flat outputs are selected to be Cartesian coordinates of the center of the wheel axle plus the relative angles that parameterize the manipulator. The trajectory tracking problem in terms of nonlinear differential equations can be transformed to algebraic equations – the later are, in general, simpler to solve than the former. The motion-planning problems can be reduced to a curve generation problem (using polynomials of appropriate order) satisfying the terminal conditions in the flat output space. The corresponding control problem can be simplified to the pole-placement problem of a linear system

to guarantee stability. Such properties are of particular interest in the field of nonholonomic mechanical system since they are, in general, not statically feedback linearizable. Finally, we demonstrate the applicability of the proposed method using hardware-in-the-loop strategy on a custom made electromechanical WMM prototype. Future work includes proposing the similar differential flatness-based motion planning/control framework for the full dynamic model of the WMM system.

ACKNOWLEDGMENTS

Tang, Miller and Krovi gratefully acknowledge the support of the NSF CAREER Award (IIS-0347653) while Ryu and Agrawal gratefully acknowledge the partial support by NSF and NIH. The authors would also like to acknowledge the contributions of Glenn White for the design and partial construction of the mechanical prototype WMM system.

REFERENCES

- [1] Velinsky, S. A., and Gardner, J. F., 2000, "Kinematics of mobile manipulators and implications for design," *Journal of Robotics Systems*, 17(6), pp. 309-320.
- [2] Stentz, A., Bares, J., Singh, S., and Rowe, P., 1999, "A Robotic Excavator for Autonomous Truck Loading," *Autonomous Robots*, 7(2), pp. 175-186.
- [3] Seraji, H., 1998, "A Unified Approach to Motion Control of Mobile Manipulators," *International Journal of Robotics Research*, 17(2), pp. 107-118.
- [4] Khatib, O., Yokoi, K., Chang, K., Ruspini, D., Holmberg, R., and Casal, A., 1996, "Vehicle/Arm Coordination and Multiple Mobile Manipulator Decentralized Cooperation," *Proceedings of the IEEE/RSJ International Conference on Intelligent Robots and Systems*, Osaka, Japan, pp. 546-553.
- [5] Bayle, B., Renaud, M., and Fourquet, J.-Y., 2003, "Nonholonomic Mobile Manipulators: Kinematics, Velocities and Redundancies," *Journal of Intelligent and Robotic Systems*, 36, pp. 45-63.
- [6] Yamamoto, Y., and Yun, X., 1994, "Coordinating Locomotion and Manipulation of a Mobile Manipulator," *IEEE Transactions on Automatic Control*, 39(6), pp. 1326-1332.
- [7] Latombe, J.-C., 1991, *Robot Motion Planning*, Kluwer Academic Publishers, Boston, MA.
- [8] Li, Z., and Canny, J. F., 1993, *Nonholonomic Motion Planning*, Kluwer Academic Publishers, Boston MA.
- [9] Bayle, B., Fourquet, J.-Y., and Renaud, M., 2003, "Manipulability of Wheeled Mobile Manipulators: Application to Motion Generation," *International Journal of Robotics Research*, 22(7-8), pp. 565-581.
- [10] Fruchard, M., Morin, P., and Samson, C., 2006, "A Framework for the Control of Nonholonomic Mobile Manipulators," *International Journal of Robotics Research*, 25(8), pp. 745-780.
- [11] Fliess, M., Levine, J., Martin, P., and Rouchon, P., 1995, "Flatness and defect of non-linear systems: Introductory theory and examples," *International Journal of Control*, 61(6), pp. 1327 - 1361.
- [12] Murray, R. M., Rathiam, M., and Sluis, W., 1995, "Differential Flatness of Mechanical Control Systems: A Catalog of Prototype Systems," *ASME International Mechanical Engineering Congress and Exposition*, San Francisco CA.
- [13] Sira-Ramirez, H., and Agrawal, S. K., 2004, *Differential Flat Systems*, Marcel Dekker, New York.
- [14] Ryu, J.-C., Agrawal, S. K., and Franch, J., 2008, "Motion Planning and Control of a Tractor with a Steerable Trailer Using Differential Flatness," *ASME Journal of Computational and Nonlinear Dynamics*, in press.
- [15] Dong, W., and Guo, Y., 2005, "New Trajectory Generation Methods for Nonholonomic Mobile Robots," *Proceedings of the International Symposium on Collaborative Technologies and Systems*, pp. 353-358.
- [16] Ryu, J.-C., Sangwan, V., and Agrawal, S. K., 2007, "Differentially Flat Designs of Mobile Vehicles with Under-actuated Manipulator Arms," *ASME International Mechanical Engineering Congress and Exposition*, Seattle WA.
- [17] White, G. D., Bhatt, R. M., and Krovi, V. N., 2008, "Experimental Evaluation of Dynamic Redundancy Resolution and Control in a Nonholonomic Wheeled Mobile Manipulator," *IEEE/ASME Transactions on Mechatronics*, in revision.
- [18] Tang, C. P., and Krovi, V., 2007, "Manipulability-Based Configuration Evaluation of Cooperative Payload Transport by Mobile Manipulator Collectives," *Robotica* 25(1), pp. 29-42.